

Galaxy flow in the Canes Venatici I cloud^{★,★★}

I. D. Karachentsev¹, M. E. Sharina^{1,11}, A. E. Dolphin², E. K. Grebel³, D. Geisler⁴, P. Guhathakurta^{5,6}, P. W. Hodge⁶,
V. E. Karachentseva⁷, A. Sarajedini⁸, and P. Seitzer⁹

¹ Special Astrophysical Observatory, Russian Academy of Sciences, N. Arkhyz, KChR 369167, Russia

² Kitt Peak National Observatory, National Optical Astronomy Observatories, PO Box 26732, Tucson, AZ 85726, USA

³ Max-Planck-Institut für Astronomie, Königstuhl 17, 69117 Heidelberg, Germany

⁴ Departamento de Física, Grupo de Astronomía, Universidad de Concepción, Casilla 160-C, Concepción, Chile

⁵ Herzberg Fellow, Herzberg Institute of Astrophysics, 5071 W. Saanich Road, Victoria, B.C. V9E 2E7, Canada

⁶ Permanent address: UCO/Lick Observatory, University of California at Santa Cruz, Santa Cruz, CA 95064, USA

⁷ Department of Astronomy, University of Washington, Box 351580, Seattle, WA 98195, USA

⁸ Astronomical Observatory of Kiev University, 04053, Observatorna 3, Kiev, Ukraine

⁹ Department of Astronomy, University of Florida, Gainesville, FL 32611, USA

¹⁰ Department of Astronomy, University of Michigan, 830 Dennison Building, Ann Arbor, MI 48109, USA

¹¹ Isaac Newton Institute, Chile, SAO Branch

Received 8 August 2002 / Accepted 25 October 2002

Abstract. We present an analysis of Hubble Space Telescope/WFPC2 images of eighteen galaxies in the Canes Venatici I cloud. We derive their distances from the luminosity of the tip of the red giant branch stars with a typical accuracy of $\sim 12\%$. The resulting distances are 3.9 Mpc (UGC 6541), 4.9 Mpc (NGC 3738), 3.0 Mpc (NGC 3741), 4.5 Mpc (KK 109), >6.3 Mpc (NGC 4150), 4.2 Mpc (UGC 7298), 4.5 Mpc (NGC 4244), 4.6 Mpc (NGC 4395), 4.9 Mpc (UGC 7559), 4.2 Mpc (NGC 4449), 4.4 Mpc (UGC 7605), 4.6 Mpc (IC 3687), 4.7 Mpc (KK 166), 4.7 Mpc (NGC 4736), 4.2 Mpc (UGC 8308), 4.3 Mpc (UGC 8320), 4.6 Mpc (NGC 5204), and 3.2 Mpc (UGC 8833). The CVn I cloud has a mean radial velocity of 286 ± 9 km s⁻¹, a mean distance of 4.1 ± 0.2 Mpc, a radial velocity dispersion of 50 km s⁻¹, a mean projected radius of 760 kpc, and a total blue luminosity of $2.2 \times 10^{10} L_{\odot}$. Assuming virial or closed orbital motions for the galaxies, we estimated their virial and their orbital mass-to-luminosity ratio to be 176 and 88 M_{\odot}/L_{\odot} , respectively. However, the CVn I cloud is characterized by a crossing time of 15 Gyr, and is thus far from a state of dynamical equilibrium. The large crossing time for the cloud, its low content of dSph galaxies ($<6\%$), and the almost “primordial” shape of its luminosity function show that the CVn I complex is in a transient dynamical state, driven rather by the free Hubble expansion than by galaxy interactions.

Key words. galaxies: dwarf – galaxies: distances and redshifts – galaxies: kinematics and dynamics – galaxies: clusters: individual: canes venatici cloud

1. Introduction

About 1/7 of the 240 known galaxies with radial velocities $V_{LG} < 400$ km s⁻¹ are concentrated in a small area in the Canes Venatici (CVn) constellation [$\alpha = 11^{\text{h}}30^{\text{m}}$ to $13^{\text{h}}40^{\text{m}}$, $\delta = +25^{\circ}$ to $+55^{\circ}$] which occupies only 1/50 of the sky. Therefore, the apparent overdensity of the number of galaxies seen in the CVn direction exceeds $\delta N/\langle N \rangle \sim 7$. This scattered complex of nearby galaxies has been noted by many authors

Send offprint requests to: M. E. Sharina,
e-mail: sme@luna.sao.ru

* Based on observations made with the NASA/ESA Hubble Space Telescope. The Space Telescope Science Institute is operated by the Association of Universities for Research in Astronomy, Inc. under NASA contract NAS 5–26555.

** Figures 1 and 2 are only available in electronic form at <http://www.edpsciences.org>

(Karachentsev 1966; de Vaucouleurs 1975; Vennik 1988). In the Nearby Galaxies Catalog (Tully 1988) the group is indicated by “14—7” (CVn I) as a part of the more extended Coma-Sculptor cloud, containing the Local Group (LG) and also the M81, Cen A, and Sculptor galaxy groups. In contrast to the groups mentioned, the CVn I cloud is populated mostly by late-type galaxies of low luminosity.

At present the structure and kinematics of the CVn I complex are still poorly understood because of the lack of reliable data on the galaxy distances. Sandage & Tammann (1982) determined the distance to IC 4182 (4.70 Mpc) from the luminosity of Cepheids. Distance estimates from the luminosity of the brightest stars were derived for DDO 154 (Carignan & Beaulieu 1989), DDO 168 (Bresolin et al. 1993) and UGC 8508 (Karachentsev et al. 1994). Using this method, Georgiev et al. (1997), Makarova et al. (1997, 1998), Karachentsev & Drozdovsky (1998), and Sharina et al. (1999) determined

distance moduli for 35 spiral and irregular galaxies in CVn I. The median distance to the cloud was found to be 4.3 Mpc, which is in good agreement with the single Cepheid distance estimate. However, considerable distance modulus errors (~ 0.5 mag) have hampered the study of structure and kinematics of the CVn I complex. That is why the CVn I objects were included in the program of our snapshot survey of nearby galaxies with the Hubble Space Telescope (Seitzer et al. 1999; Grebel et al. 2000), where galaxy distances are determined on the basis of a much more precise method, via the luminosity of red giant branch tip stars. In the framework of this study of galaxies in the Local Volume we earlier investigated the Centaurus A group (Karachentsev et al. 2002a) and the M81 group (Karachentsev et al. 2000, 2001, 2002b). The first distance measurements for five members of the Cloud based on the HST data have already been published (Karachentsev et al. 2002c). Here, we present new distances for 18 galaxies in the CVn I area.

2. WFPC2 photometry

The galaxy images were obtained with the Wide Field and Planetary Camera (WFPC2) aboard the Hubble Space Telescope (HST) between July 23, 1999 and June 20, 2001 as part of our HST snapshot survey (proposals GO 8192, 8601) of nearby galaxy candidates (Seitzer et al. 1999). Each galaxy was observed in the F606W and F814W filters (one 600 s exposure in each filter). Digital Sky Survey images of the galaxies are shown in Fig. 1 with the HST WFPC2 footprints superimposed. Small galaxies were usually centered on the WF3 chip. For some bright objects the WFPC2 position was shifted towards the galaxy periphery to decrease stellar crowding. The WFPC2 images of the galaxies are presented in the upper panels of Fig. 2, where both filters are combined. The compass in each field indicates the North and East directions.

For photometric measurements we used the HSTphot stellar photometry package developed by Dolphin (2000a). The package has been optimized for the undersampled conditions present in the WFPC2 to work in crowded fields. After removing cosmic rays, simultaneous photometry was performed on the F606W and F814W frames using *multiphot* task. The resulting instrumental magnitudes were measured with an aperture radius of $0''.5$ and corrected for charge-transfer inefficiency. Then they were converted to standard V and I magnitudes using the relations (11) and (12) of Dolphin (2000b). These calibration equations are analogous to equations of Holtzman et al. (1995), but incorporate the pixel area corrections. Additionally, stars with a signal-to-noise ratio $S/N < 3$, $|\chi| > 2.0$, or $|\text{sharpness}| > 0.4$ in either exposure were eliminated from the final photometry list. The uncertainty of the photometric zero point is estimated to be within $0^m.05$ (Dolphin 2000b).

3. CMDs and galaxy distances

During the last decade the tip of the red giant branch (TRGB) method has become an efficient tool for measuring galaxy distances. The TRGB distances agree with the distances derived

from the Cepheid period-luminosity relation within a 5% error. As was shown by Lee et al. (1993), Salaris & Cassisi (1997), and Udalski et al. (2001), in the I band the TRGB position is relatively independent of age and metallicity within ~ 0.1 mag for old stellar populations with $[\text{Fe}/\text{H}] < -0.7$ dex. According to Da Costa & Armandroff (1990), for metal-poor systems the TRGB is located at $M_I = -4.05$ mag. Ferrarese et al. (2000) calibrated the zero point of the TRGB from galaxies with Cepheid distances and yielded $M_I = -4.06 \pm 0.07$. A new TRGB calibration $M_I = -4.04 \pm 0.12$ mag was determined by Bellazzini et al. (2001) based on photometry and distance estimation from a detached eclipsing binary in the Galactic globular cluster ω Centauri. In the present paper we adopt $M_I = -4.05$ mag. The bottom left panels of Fig. 2 show I versus $(V-I)$ color-magnitude diagrams (CMDs) for the eighteen observed galaxies.

We determined the TRGB location using a Gaussian-smoothed I -band luminosity function (LF) for red stars with colors $(V-I)$ within $\pm 0^m.5$ of the mean $\langle V-I \rangle$ for expected red giant branch stars. Following Sakai et al. (1996), we applied a Sobel edge-detection filter. The position of the TRGB was identified with the peak in the filter response function. The resulting LFs and the Sobel-filtered LFs are shown in the bottom right corners of Fig. 2. The results are summarized in Table 1. This table contains the following columns: (1) galaxy name; (2) equatorial coordinates corresponding to the galaxy center; (3,4) angular size in arcmin and apparent total magnitude from the NASA Extragalactic Database (NED), uncorrected for internal and external extinction; (5) Galactic extinction in the B , I -bands from Schlegel et al. (1998); (6) integrated or effective color of the galaxy, corrected for Galactic extinction; the data on colors are taken from Makarova et al. (1998), Makarova (1999), and Prugniel & Heraudeau (1998); for the galaxies NGC 3741, KK 109, and KK 166 we present $V-I$ colors of their core from our measurements; (7) morphological type in de Vaucouleurs notation; (8) radial velocity with respect to the LG centroid; for some galaxies we used new accurate velocities measured recently by Huchtmeier et al. (2002); (9) position of the TRGB and its uncertainty derived with the Sobel filter; (10) true distance modulus with its uncertainty, which takes into account the uncertainty in the TRGB detection as well as uncertainties of the HST photometry zero point ($\sim 0^m.05$), the aperture corrections ($\sim 0^m.05$), and crowding effects ($\sim 0^m.06$) added in quadrature; uncertainties in extinction and reddening are assumed to be 10% of their values from Schlegel et al. (1998); and (11) linear distance in Mpc and its uncertainty.

Given the distance moduli of the galaxies, we can estimate their mean metallicity, $[\text{Fe}/\text{H}]$, from the mean color of the TRGB measured at an absolute magnitude $M_I = -3.5$, as recommended by Da Costa & Armandroff (1990). Based on a Gaussian fit to the color distribution of the giant stars in a corresponding I -magnitude interval (-3.5 ± 0.3), we derived their mean colors, $(V-I)_{-3.5}$, which lie in a range of $[1.15-1.68]$ after correction for Galactic reddening. Following the relation of Lee et al. (1993), this provides us with mean metallicities, $[\text{Fe}/\text{H}] = [-0.8, -2.5]$ dex, listed in the last column of Table 1. With a typical statistical scatter of the mean color ($\sim 0^m.05$), and

Table 1. New distances to galaxies in the Canes Venatici cloud.

Name	RA (1950) Dec hh mm ss ° ° ' ''	$a \times b$ '	B_t mag	A_b A_i	$(V - I)_T$ $\pm \sigma$	T	V_{LG} km s^{-1}	$I(\text{TRGB})$ mag	$(m - M)_o$ mag	D Mpc	$(V - I)_{-3.5}$ [Fe/H]
U6541	113045.2 493043	1.4×0.8	14.23	0.08 0.04	0.53 ± 0.07	10	304	23.94 ± 0.28	27.95 ± 0.29	3.89 ± 0.47	1.39 -1.54
N3738	113304.4 544758	2.6×1.9	12.13	0.05 0.02	0.62 ± 0.10	10	305	24.42 ± 0.24	28.45 ± 0.25	4.90 ± 0.54	1.48 -1.27
N3741	113325.2 453343	2.0×1.1	14.3	0.10 0.05	0.67 ± 0.10	10	264	23.41 ± 0.21	27.41 ± 0.23	3.03 ± 0.33	1.37 -1.61
KK109	114433.5 435659	0.6×0.4	18.62	0.08 0.04	0.80 ± 0.10	10	241	24.26 ± 0.15	28.27 ± 0.17	4.51 ± 0.34	1.15 -2.54
N4150	120801.2 304054	2.3×1.6	12.45	0.08 0.04	1.20 ± 0.01	-1	198	-	-	20:	-
U7298	121400.6 523018	1.1×0.6	15.95	0.10 0.05	0.45 ± 0.26	10	255	24.12 ± 0.15	28.12 ± 0.17	4.21 ± 0.32	1.32 -1.80
N4244	121459.8 380506	19.4×2.1	10.67	0.09 0.04	0.89 ± 0.07	6	255	24.25 ± 0.22	28.26 ± 0.24	4.49 ± 0.47	1.32 -1.80
N4395	122320.8 334922	13.2×11.0	10.61	0.07 0.03	0.73 ± 0.11	9	315	24.30 ± 0.28	28.32 ± 0.29	4.61 ± 0.57	1.45 -1.36
U7559 DDO126	122437.1 372509	3.2×2.0	14.12	0.06 0.03	0.48 ± 0.10	10	231	24.42 ± 0.24	28.44 ± 0.26	4.87 ± 0.55	1.29 -1.91
N4449	122545.1 442215	6.2×4.4	9.83	0.08 0.04	0.63 ± 0.02	10	249	24.11 ± 0.26	28.12 ± 0.27	4.21 ± 0.50	1.43 -1.42
U7605	122611.0 355940	1.1×0.8	14.76	0.06 0.03	0.61 ± 0.10	10	317	24.21 ± 0.27	28.23 ± 0.28	4.43 ± 0.53	1.21 -2.26
IC3687 DDO141	123950.8 384633	3.4×3.0	13.75	0.09 0.04	0.57 ± 0.26	10	385	24.29 ± 0.22	28.30 ± 0.24	4.57 ± 0.48	1.32 -1.80
KK166	124649.5 355305	1.7×1.0	17.62	0.06 0.03	1.20 ± 0.2	-3	-	24.36 ± 0.34	28.38 ± 0.34	4.74 ± 0.69	1.27 -2.00
N4736 M94	124832.3 412328	11.2×9.1	8.74	0.08 0.04	1.19 ± 0.01	2	353	24.33 ± 0.28	28.34 ± 0.29	4.66 ± 0.59	1.69 -0.84
U8308 DDO167	131110.0 463511	1.1×0.6	15.53	0.04 0.02	0.69 ± 0.26	10	243	24.08 ± 0.25	28.11 ± 0.26	4.19 ± 0.47	1.37 -1.61
U8320 DDO168	131216.6 461101	3.6×1.4	12.73	0.07 0.03	0.52 ± 0.26	10	273	24.16 ± 0.25	28.18 ± 0.26	4.33 ± 0.49	1.28 -1.96
N5204	132743.8 584032	5.0×3.0	11.73	0.05 0.02	0.75 ± 0.01	9	341	24.31 ± 0.26	28.34 ± 0.27	4.65 ± 0.53	1.32 -1.80
U8833	135236.0 360500	0.9×0.8	15.15	0.05 0.02	0.68 ± 0.10	10	285	23.49 ± 0.12	27.52 ± 0.15	3.19 ± 0.21	1.26 -2.04

the uncertainty of the HST photometry zero point we expect an uncertainty in metallicity to be about 0.3 dex. Therefore within the measurement accuracy the metallicity of the galaxies satisfy the required limitation, $[\text{Fe}/\text{H}] < -0.7$ dex.

Below, some individual properties of the galaxies are briefly discussed.

UGC 6541 = Mkn 178. A blue compact galaxy from Markarian's lists is located on the NW edge of the CVnI cloud. It was resolved into stars for the first time by Georgiev et al. (1997), who derived a distance of 3.5 ± 0.7 Mpc via the

brightest blue stars. The distance to UGC 6541 from the luminosity of TRGB is $D = 3.89 \pm 0.47$ Mpc, which is in reasonable agreement with the previous estimate.

NGC 3738 = UGC 6565 = Arp 234. This dwarf irregular galaxy appears to be semi-resolved into brightest stars on the reproduction given in the Atlas of Peculiar Galaxies (Arp 1966). Georgiev et al. (1997) estimated its distance as 3.5 ± 0.7 Mpc from the magnitudes of the brightest blue stars. The images obtained with WFPC2 reveal about 17 700 stars seen in both filters. The CM diagram for NGC 3738 shows

a large number of blue stars, as well as AGB stars. From the TRGB position we derive a distance of 4.90 ± 0.54 Mpc.

NGC 3741 = UGC 6572. Like two previous objects, NGC 3741 lies at the NW periphery of the CVnI cloud. The galaxy has an asymmetric “cometary” shape. Its size in H I exceeds its optical diameter significantly (Haynes & Giovanelli 1991). Georgiev et al. (1997) derived its distance to be 3.5 ± 0.7 Mpc from the brightest blue stars, while the TRGB distance from our measurements is 3.03 ± 0.33 Mpc.

KK 109. This dwarf irregular galaxy of low surface brightness was found by Karachentseva & Karachentsev (1998). Huchtmeier et al. (2000) detected it in the H I line and determined its radial velocity, $V_{LG} = 241 \text{ km s}^{-1}$, which is typical for CVnI members. The CM diagram of KK 109 shows the TRGB magnitude to be 24.26 ± 0.15 mag, which yields a distance of 4.51 ± 0.34 Mpc. Based on the WFPC2 images, we carried out surface photometry of KK 109, obtaining total magnitudes $V_t = 18.14 \pm 0.2$ mag, $(V - I)_t = 0.8 \pm 0.1$ mag, and a central surface brightness of $23.6 \pm 0.2 \text{ mag arcsec}^{-2}$ in the V band. With the derived apparent magnitude and distance, KK 109 has an absolute magnitude of $M_V = -10.19$ mag, placing it among the faintest known dIrr galaxies such as LGS 3 and Antlia.

NGC 4150. The core of this lenticular galaxy is crossed by a curved dusty furrow (see insert in Fig. 2). In spite of its low radial velocity, $V_{LG} = 198 \text{ km s}^{-1}$, NGC 4150 appears unresolved into stars on the WFPC2 images. Its TRGB magnitude appears to exceed $I_{lim} = 25$ mag (beyond our detection limit), yielding a lower limit of 6.3 Mpc for its distance. We suggest that NGC 4150 belongs to the Virgo cluster outskirts, and not to the CVnI cloud. Most of the objects seen in the galaxy body seem to be slightly extended and diffuse with integrated colors of $V - I = 0.8\text{--}1.6$, which raises the possibility that they are globular clusters. If they are indeed globular clusters, we can use the turnover magnitude of the globular cluster luminosity function (GCLF), $V \sim 24$ mag, as a distance indicator (Ferrarese et al. 2000). With this assumption we derive a rough distance estimate of ~ 20 Mpc consistent with the Virgo cluster distance.

UGC 7298. This is a dIrr galaxy of low surface brightness. UGC 7298 has been resolved into stars by Tikhonov & Karachentsev (1998), who estimated its distance to be 8.6 ± 1.5 Mpc via the brightest stars. The CM diagram (Fig. 2) shows populations of blue stars and AGB stars. We determine the TRGB magnitude to be $I(\text{TRGB}) = 24.12 \pm 0.15$ mag, which gives a distance of 4.21 ± 0.32 Mpc. The TRGB distance is approximately two times smaller than the distance from the brightest stars. A possible cause of this difference is a lack of very luminous blue stars in this galaxy, i.e., no very recent massive star formation.

NGC 4244. A large edge-on Sc galaxy extends far beyond the WFPC2 field. Its periphery was resolved into stars by Karachentsev & Drozdovsky (1998), who estimated the galaxy distance to be 4.5 ± 0.9 Mpc from the photometry of the brightest stars. The CM diagram (Fig. 2) shows $\sim 15\,000$ stars, in particular pronounced populations of blue stars and AGB stars. The TRGB position, 24.25 ± 0.22 mag, corresponds to a

distance of 4.49 ± 0.47 Mpc in close agreement with the distance estimate via the brightest stars.

NGC 4395. This face-on Sd galaxy with a Seyfert 1 type nucleus also extends beyond the WFPC2 field. According to Karachentsev & Drozdovsky (1998), its distance via the brightest blue stars is 4.2 ± 0.8 Mpc. The CM diagram in Fig. 2 reveals about 21 800 stars seen both in the V and I bands. The majority of the detected stars are likely RGB stars. From the TRGB position we derive a distance of 4.61 ± 0.57 Mpc, which agrees well with the previous distance estimate.

UGC 7559 = DDO 126. This irregular dwarf galaxy has been resolved into stars by Hopp & Schulte-Ladbeck (1995), Georgiev et al. (1997), and Makarova et al. (1998), who derived distance estimates of 4.8 Mpc, 3.9 Mpc, and 5.1 Mpc, respectively. Our distance for UGC 7559 based on the TRGB (4.87 ± 0.55 Mpc) is in the middle of the range previously obtained by other authors.

NGC 4449. This boxy-shaped Magellanic irregular galaxy of high surface brightness is a second ranked member of the CVnI cloud according to its luminosity. NGC 4449 is enveloped in a huge H I “fur coat”, whose angular size ($75'$) exceeds the Moon’s diameter (Bajaja et al. 1994). Based on photometry of the brightest stars, Karachentsev & Drozdovsky (1998) estimated its distance to be 2.9 ± 0.6 Mpc. The WFPC2 photometry reveals about 27 000 stars seen in both images. The CM diagram in Fig. 2 shows stellar populations of different kinds including RGB stars. From the TRGB magnitude, 24.11 ± 0.26 mag, we derive a distance of 4.21 ± 0.50 Mpc.

UGC 7605. This is a blue irregular galaxy shaped like a horseshoe. The brightest blue stars in UGC 7605 are concentrated towards the core, and the outlying galaxy parts are redder and smoother. From the luminosity of the brightest stars Makarova et al. (1998) derived a galaxy distance of 4.4 ± 0.9 Mpc. The CM diagram of UGC 7605 (Fig. 2) shows the RGB population giving a distance of 4.43 ± 0.53 Mpc, which is in close agreement with the previous estimate.

IC 3687 = DDO 141 = UGC 7866. IC 3687 is an irregular dwarf galaxy with several regions of current star formation activity. Its CM diagram shows a mixed stellar population with a pronounced RGB with $I(\text{TRGB}) = 24.29 \pm 0.22$ mag, which corresponds to a distance of 4.57 ± 0.48 Mpc. Our distance for IC 3687 differs from the previous distance, 3.0 ± 0.6 Mpc, obtained by Makarova et al. (1998) via the brightest stars.

KK 166. This galaxy is unique in terms of being the only dwarf spheroidal (dSph) galaxy of very low surface brightness identified so far in the CVnI region. (Another possible dSph in CVnI is DDO 113 = KDG 90.) The galaxy has been observed but not detected in the H I line by Huchtmeier et al. (2000). The CM diagram shows a dominant RGB population with $I(\text{TRGB}) = 24.36 \pm 0.34$ mag, yielding a distance of 4.74 ± 0.69 Mpc, which confirms KK 166 as a likely member of the CVnI cloud. Apart from stellar photometry, we also carried out surface photometry in circular apertures. From our measurements KK 166 has a total magnitude $V_t = 16.8 \pm 0.2$ mag, $(V - I)_t = 1.2 \pm 0.1$ mag, and a central surface brightness of $25.0 \pm 0.2^m/\square''$ in the V band.

NGC 4736 = M 94. NGC 4736 is the brightest galaxy of type Sa in CVnI. We resolve it into stars for the first time.

The WFPC2 was pointed at the galaxy periphery to avoid stellar crowding. In the galaxy halo the CM diagram (Fig. 2) shows numerous RGB stars with $I(\text{TRGB}) = 24.33 \pm 0.28$ mag, which yields a distance of 4.66 ± 0.59 Mpc. Karachentseva & Karachentsev (1998) carried out a proper search for dwarf companions to NGC 4736 based on the POSS-II plates. Surprisingly, they found no companions with a central surface brightness brighter than $25^m/\square''$ in the B band within a radius of ~ 3 degrees or 230 kpc around this giant galaxy. Such a pronounced degree of isolation of an Sa galaxy situated in the middle of the CVn I cloud seems rather unusual.

UGC 8308 = DDO 167. This is an asymmetric irregular galaxy of low surface brightness, becoming redder from its core to the periphery. It has been resolved into stars by Tikhonov & Karachentsev (1998), who derived a distance of 3.7 ± 0.7 Mpc from the brightest star photometry. The CMD (Fig. 2) shows blue and red stellar populations with the TRGB position yielding a distance of 4.19 ± 0.47 , which is in close agreement with the previous estimate.

UGC 8320 = DDO 168. This irregular galaxy is located 14' away from UGC 8308, forming a probable pair of dwarf galaxies. Bresolin et al. (1993), Hopp & Schulte-Ladbeck (1995), and Tikhonov & Karachentsev (1998) have resolved it into stars and estimated its distance to be 3.3 Mpc, 3.9 Mpc, and 4.0 Mpc, respectively. The WFPC2 photometry gives a TRGB magnitude corresponding to a distance of 4.33 ± 0.49 Mpc. The derived TRGB distances of UGC 8320 and UGC 8308 agree with each other within the uncertainties.

NGC 5204. NGC 5204 is an irregular galaxy of Magellanic type, which is located at the northern edge of the CVn I cloud. Its distance, 4.9 ± 1.0 Mpc, was estimated by Karachentsev et al. (1994) via the brightest blue and red stars. The CM diagram (Fig. 2) shows a mixed stellar population with a prominent RGB. The derived TRGB distance, 4.65 ± 0.53 Mpc, is in good agreement with the previous estimate.

UGC 8833. This blue irregular galaxy looks like a binary system because of several regions with ongoing intense star formation. UGC 8833 is situated at the eastern edge of the CVn I cloud. According to Makarova et al. (1998) its distance derived from its brightest stars is 3.2 ± 0.6 Mpc. Our photometry of the WFPC2 images yields a TRGB distance of 3.19 ± 0.21 Mpc, which confirms the previous distance estimate.

4. Properties of the Canes Venatici I cloud

Figure 3 presents the distribution of 223 galaxies within an area of $\alpha = 11^{\text{h}}30^{\text{m}}$ to $13^{\text{h}}40^{\text{m}}$, $\delta = 25^\circ$ to 55° according to their radial velocities with respect to the LG centroid. The data are taken from the latest version of the Lyon Extragalactic Database (LEDa) prepared by Paturel et al. (1996). The histogram shows a rather isolated peak at $V_{\text{LG}} = 200\text{--}350$ km s $^{-1}$, which is caused by galaxies in the CVn I cloud. Another peak is seen in the range of $500\text{--}650$ km s $^{-1}$ and may correspond to a more distant galaxy group aligned along the Supergalactic equator (data on distances of these galaxies are yet unknown). The distribution of 72 galaxies with $V_{\text{LG}} < 550$ km s $^{-1}$ is given in equatorial coordinates in Fig. 4. The galaxies with $V_{\text{LG}} < 400$ km s $^{-1}$ are shown by filled circles. Two brightest

members of the CVn I cloud, NGC 4736 and NGC 4449, are indicated by filled squares. Probable background galaxies with $400 < V_{\text{LG}} < 550$ km s $^{-1}$ are shown by crosses. The complete list of the galaxies is given in Table 2. Its columns contain: (1) galaxy name, (2) equatorial coordinates (1950.0), (3) apparent blue magnitude from the NED (uncorrected for Galactic extinction), (4) morphological type, (5) radial velocity with respect to the LG centroid, (6) distance to the galaxy with indication of the used method: “Cep” – via cepheids, “RGB” – via the tip of red giant branch stars, “SBF” – via surface brightness fluctuations, “BS” – from the luminosity of the brightest stars, and “GCLF” – via the globular cluster luminosity function. The last column presents the source of data on the distance. In addition, we included in Table 2 an interacting galaxy pair NGC 5194/5195 with an accurate distance estimate and three nearby dwarf galaxies: DDO 187, DDO 190, and KK 230, situated slightly to the east of the above indicated boundary of the cloud. The data given in Figs. 3 and 4, and Table 2 permit us to infer properties of the structure and kinematics of the CVn I cloud.

Judging from their distances and radial velocities, 34 galaxies may be CVn I members. We distinguish their names in Table 2 with bold print. Among them there are 24 galaxies whose distances have been measured with an accuracy of $\sim(10\text{--}15)\%$. For the other 10 probable members of CVn I only rough distance estimates via the brightest stars are known so far. Karachentsev & Tikhonov (1994) claimed the typical error of distance modulus for the “BS”-method to be 0.4 mag. However, Rozanski & Rowan-Robinson (1994) and some others considered the uncertainties of this method to be greater than 0.5 mag. In Table 2 there are 19 galaxies whose distances have been measured at first via the brightest stars and then via TRGB. Their distance moduli are given in Table 3. Apart from three cases (UGC 7298, UGC 7577, and UGCA 290) with $\Delta(m - M)$ larger than 1.0 mag, the mean difference of distance moduli for the remaining 16 galaxies is $\langle (m - M)_{\text{BS}} - (m - M)_{\text{RGB}} \rangle = -0.08 \pm 0.12$ mag, and the rms difference is 0.48 mag. As can be seen from Table 2, apart from galaxies with rough distance estimates there are also many galaxies whose distances have not yet been measured at all. For some objects (PGC 38277, PGC 38685, PGC 91228) their unreliable velocity estimates need to be checked. Due to the incompleteness of the present set of observational data, our conclusions about the structure of the CVn I cloud will have a preliminary character.

Unlike the Local Group and the nearest groups around M81 and Cen A, the galaxy complex in CVn I has no distinct dynamical center usually designated by a giant early-type galaxy. We assume that the dynamical center of CVn I lies between the two brightest cloud members, NGC 4736 and NGC 4449. Their absolute magnitudes, -19.69 and -18.37 mag, are substantially fainter than those of the Milky Way, M 31, M 81, and Centaurus A. As was mentioned above, around the Sa galaxy NGC 4736 there is not any known dwarf galaxy within 230 kpc. Such isolateness of NGC 4736 distinguishes it from the brightest members of other groups. If the luminosity of the brightest member of any group depends on the merging process of

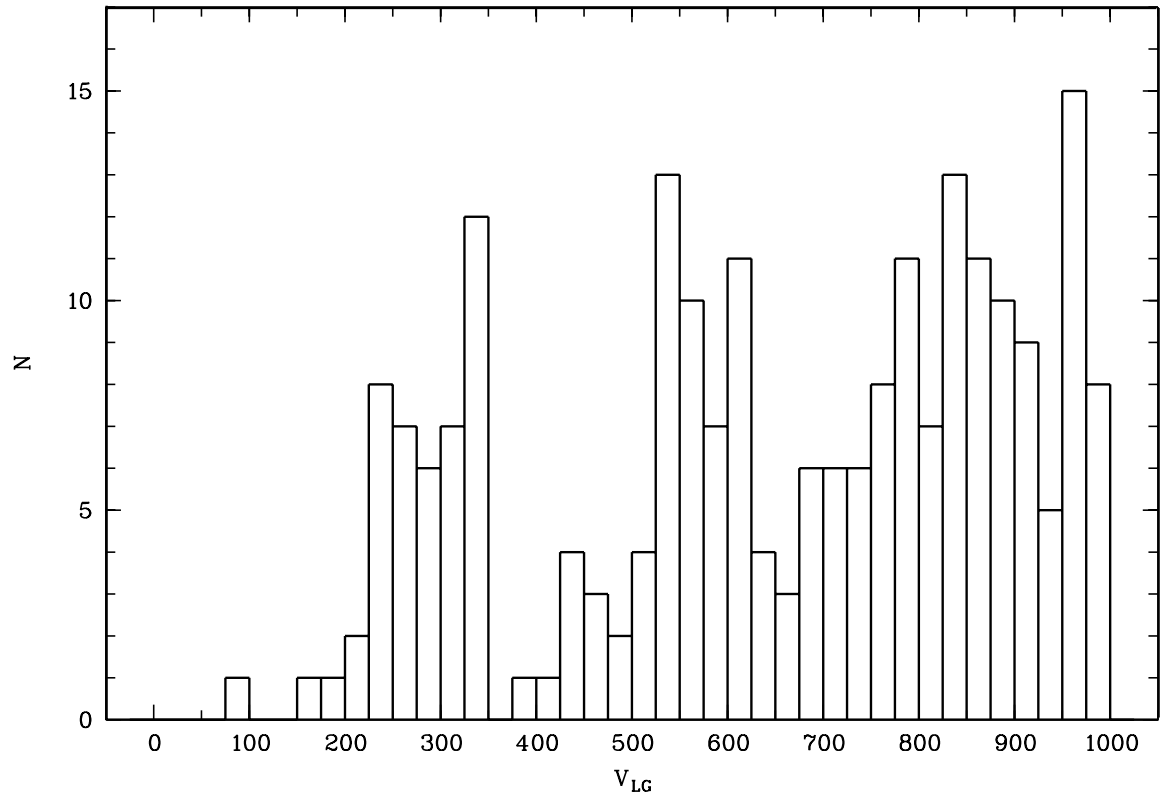


Fig. 3. Radial velocity distribution of 223 galaxies in the CVn I region.

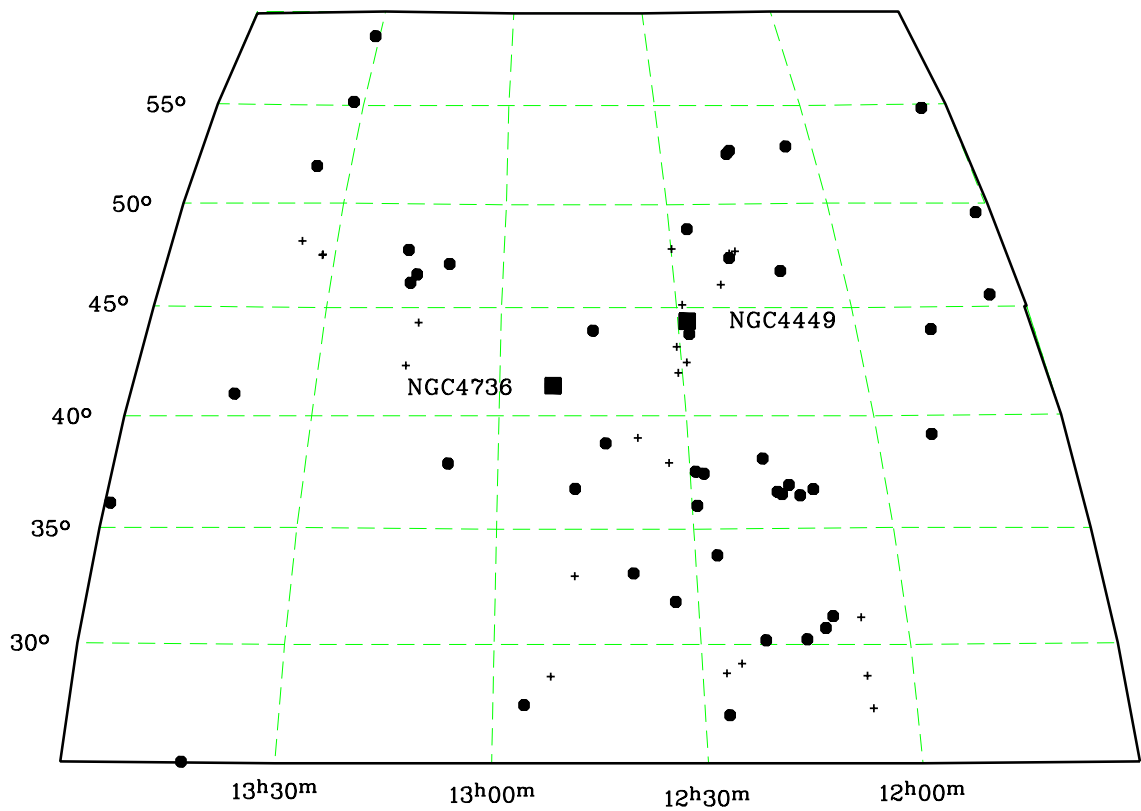


Fig. 4. The distribution of 72 galaxies with corrected radial velocities $V_{LG} < 550 \text{ km s}^{-1}$ in the Canes Venatici constellation in equatorial coordinates. The galaxies with $V_{LG} < 400 \text{ km s}^{-1}$ and $>400 \text{ km s}^{-1}$ are indicated by filled circles and crosses, respectively. The two brightest galaxies, NGC 4736 and NGC 4449, are shown by filled squares.

Table 2. Galaxies in the Canes Venatici region with $V_{LG} < 550 \text{ km s}^{-1}$.

Name	RA (B1950) Dec	B_t	T	V_{LG}	Distance	Reference
U6541	113045.9 493052	14.23	10	304	3.89 RGB	present paper
N3738	113304.4 544758	12.13	10	305	4.90 RGB	present paper
N3741	113325.2 453343	14.3	10	264	3.03 RGB	present paper
KK109	114433.5 435659	18.62	10	241	4.51 RGB	present paper
U6817	114816.8 390931	13.44	10	248	2.64 RGB	Karachentsev et al. (2002c)
N4068	120129.7 525201	13.19	10	290	5.2 BS	Makarova et al. (1997)
N4080	120218.6 271616	14.28	10	519		
Mrk757	120242.9 310801	14.80	0:	551		
P38286	120250.2 283839	15.36	10	527		
U7131	120639.4 311106	15.50	8	226	14. BS	Makarova et al. (1998)
P38685	120724.5 364248	15.5	9:	341		
N4144	120728.2 464407	12.16	6	319	9.7 BS	Karachentsev et al. (1998)
N4150	120801.4 304047	12.45	-2	198	20: GCLF	present paper
N4163	120937.5 362651	13.93	10	164	3.6 BS	Tikhonov et al. (1998)
KK127	121051.0 301159	15.61	10	105		
N4190	121113.5 365440	13.52	10	234	3.5 BS	Tikhonov & Karachentsev (1998)
KDG90	121227.1 362948	15.40	-1	283	2.86 RGB	Karachentsev et al. (2002c)
N4214	121308.2 363619	10.24	10	295	2.94 RGB	Maiz-Apellaniz et al. (2002)
P39228	121318.5 523955	15.3	10	245		
U7298	121400.6 523018	15.95	10	255	4.21 RGB	present paper
N4244	121459.8 380506	10.67	6	255	4.49 RGB	present paper
N4248	121523.0 474109	13.12	9:	544		
N4258	121629.4 473453	9.10	4	507	7.28 SBF	Tonry et al. (2001)
U7356	121641.0 472202	15.10	10	330:		(HI flux confusion?)
U7369	121708.1 300938	14.70	-1	198		
U7408	121847.5 460520	13.35	10	515		
IC3247	122043.8 291015	15.25	8	539		
IC3308	122247.7 265929	15.17	7	277		
KK144	122258.0 284533	16.5	10	453		
N4395	122320.8 334922	10.61	9	315	4.61 RGB	present paper
UA281	122350.5 484607	15.15	10	349	5.7 BS	Makarova et al. (1997)
U7559	122437.1 372509	14.12	10	231	4.87 RGB	present paper
U7577	122515.4 434613	12.84	10	240	2.54 RGB	Karachentsev et al. (2002c)
N4449	122545.1 442215	9.83	10	249	4.21 RGB	present paper
U7599	122600.8 373035	14.98	9	291	6.9 BS	Makarova et al. (1998)
U7605	122611.0 355940	14.76	10	317	4.43 RGB	present paper

surrounding dwarf galaxies, then the rate of the merging process in the CVn I cloud was slow.

The amorphous cloud CVn I differs essentially from more compact nearby groups by its very sparse population of dSph galaxies. Only one CVn I member, KK 166, may currently be considered to be a definitive dSph galaxy. Another reddish LSB dwarf galaxy of regular shape, KDG 90, shows a strong H I flux, not typical of the dSphs. However, KDG 90 is situated near the bright irregular galaxy NGC 4214, which may lead to H I flux confusion. Anyhow, the relative number of dSphs in CVn I does not exceed 6%, which also gives evidence of low rate of interaction between the cloud galaxies if dSphs are primarily the result of stripping in interactions.

Comparing the luminosity function (LF) for field galaxies with the LF for members of three nearest groups (LG + M 81 + Cen A), Karachentsev et al. (2002c) noted an excess of very faint ($M_B > -12$ mag), as well as giant ($M_B < -20$ mag) galaxies in the groups. The excess of galaxies of extreme luminosities may be understood if the primordial LF grows on its bright and faint ends owing to “cannibalism” and “debris” left

by galaxy interactions. In Fig. 5 we present the LF for 34 members of the CVn I cloud together with the LFs for 38 field galaxies and 96 members of the three groups. As it follows from Fig. 5, the LF of the CVn I seems to resemble the field LF more closely than the group LF. This feature indicates once again that galaxy interactions do not necessarily exercise significant influence on the dynamical evolution of galaxies in the CVn I cloud.

As was mentioned above, the boundary and the center position of the CVn I cloud still remain uncertain. Based on the data of Fig. 4 and Table 2, one can speculate that the cloud is a superposition of several groups populated by almost entirely irregular dwarf galaxies. In that sense, the CVn I complex resembles another loose cluster of late-type galaxies in Cancer (Bicay & Giovanelli 1987) and nearby cloud of dIrr galaxies in Ursa Major (Tully et al. 1996). Some groups in CVn I, for instance, [NGC 4244, NGC 4395, UGC 7559, UGC 7605, IC 3687], [UGC 8215, UGC 8308, UGC 8320, UGC 8331], and [UGC 8651, UGC 8760, UGC 8833] fit the definition of groups of “squelched” galaxies introduced by

Table 2. continued.

Name	RA (B1950) Dec	B_t	T	V_{LG}	Distance	Reference
N4460	122620.0 450827	12.26	-1	542	9.59 SBF	Tonry et al. (2001)
KK149	122625.8 422715	15.01	10	446		
U7639	122728.4 474822	14.13	10	446	8.0 BS	Makarova et al. (1998)
KK151	122758.0 431039	15.8	9	479		
N4485	122805.1 415833	12.32	10	530		
U7699	123021.5 375352	13.17	8	514		
U7698	123024.9 314853	13.15	10	321	6.1 BS	Makarova et al. (1998)
UA290	123456.0 390112	15.74	10	484	6.70 RGB	Crone et al. (2002)
UA292	123613.3 330229	16.1	10	306	3.1 BS	Makarova et al. (1998)
IC3687	123950.8 384633	13.75	10	385	4.57 RGB	present paper
KK160	124135.0 435615	17.	10	346		
FGC1497	124435.2 325521	16.	9	521		
U7949	124435.9 364457	15.12	10	351	10. BS	Makarova et al. (1998)
KK166	124649.5 355305	17.62	-3		4.74 RGB	present paper
U7990	124801.0 283726	16.2	10	495		
N4736	124832.3 412328	8.74	2	353	4.66 RGB	present paper
U8024	125139.3 272510	14.17	10	355	4.3 BS	Makarova et al. (1998)
IC4182	130329.9 375223	12.41	9	356	4.70 Cep	Sandage & Tammann (1982)
U8215	130550.4 470524	16.07	10	297	5.6 BS	Makarova et al. (1997)
N5023	130957.9 441813	12.82	6	476	5.4 BS	Sharina et al. (1999)
U8308	131110.8 463504	15.53	10	243	4.19 RGB	present paper
KK191	131124.0 421831	18.2	10	429		
U8320	131216.6 461101	12.73	10	273	4.33 RGB	present paper
U8331	131320.3 474537	14.61	10	345	8.2 BS	Karachentsev & Drozdovsky (1998)
N5204	132743.8 584032	11.73	9	341	4.65 RGB	present paper
N5194	132749.7 472932	8.57	5	555	7.7 mem	pair with N5195
N5195	132752.4 473132	10.45	-1	558	7.66 SBF	Tonry et al. (2001)
U8508	132847.1 551002	14.40	10	186	2.56 RGB	Karachentsev et al. (2002c)
N5229	133158.5 481016	14.51	7	460	5.1 BS	Sharina et al. (1999)
N5238	133242.6 515209	13.8	8	345	5.2 BS	Karachentsev & Tikhonov (1994)
U8638	133658.5 250144	14.47	10	273	2.3: BS	Makarova et al. (1998)
U8651	133744.2 405931	14.7	10	272	3.01 RGB	Karachentsev et al. (2002c)
U8833	135236.0 360500	15.15	10	285	3.19 RGB	present paper
KK230	140501.5 351809	17.9	10	125	1.90 RGB	Grebel et al. (2001)
DDO187	141338.6 231713	14.38	10	174	2.50 RGB	Aparicio et al. (2000)
DDO190	142248.7 444506	13.25	10	266	2.79 RGB	Karachentsev et al. (2002c)

Tully et al. (2002). Luminous matter in such groups plays a negligible role in their dynamical evolution.

5. Kinematics of the CVn I cloud

The sample of 34 possible members of the CVn I cloud, which are marked in Table 2 in bold print, are characterized by a mean distance $\langle D \rangle = 4.1 \pm 0.2$ Mpc and a mean radial velocity $\langle V_{LG} \rangle = 286 \pm 9$ km s⁻¹. The ratio of these quantities yields $H(CVnI) = 70 \pm 4$ km s⁻¹ Mpc⁻¹ as the local value of the Hubble constant, which agrees well with its global value, $H_0 = 69 \pm 4$ (random) ± 6 (systematic) km s⁻¹ Mpc⁻¹ (Ferrarese et al. 2000). In other words, within the uncertainties the CVn I cloud as a whole is at rest with respect to the global cosmic flow within random errors.

As a dynamical system, the CVn I cloud has the following integrated parameters: a radial velocity dispersion $\sigma_v = 50$ km s⁻¹, a mean projected linear radius $\langle R_p \rangle = 760$ kpc, a mean harmonic projected radius $\langle R_H \rangle = 635$ kpc, and an integrated luminosity of $L_B = 2.15 \times 10^{10} L_\odot$. Considering the

CVn I cloud to be in dynamical equilibrium and applying the virial relation (Limber & Mathews 1960)

$$M_{\text{vir}} = 3\pi N \cdot (N - 1)^{-1} \cdot G^{-1} \cdot \sigma_v^2 \cdot R_H,$$

where G is the gravitational constant and N is the number of group members, we obtain the virial mass estimate

$$M_{\text{vir}} = 3.6 \times 10^{12} M_\odot$$

and the virial mass-to-total luminosity ratio of $167 M_\odot/L_\odot$. Because half of the total luminosity of the CVnI cloud is emitted by its brightest galaxy, NGC 4736, we may consider formally the remaining cloud members as companions to NGC 4736. Under these assumptions, the orbital mass estimator is

$$M_{\text{orb}} = (32/3\pi) \cdot G^{-1} \cdot (1 - 2e^2/3)^{-1} \langle R_p \cdot \Delta V_r^2 \rangle,$$

where e is the eccentricity of the Keplerian orbit, and R_i and ΔV_i are the projected linear distance and radial velocity of a companion with respect to NGC 4736. Adopting a mean eccentricity $e = 0.7$, we derive $M_{\text{orb}} = 1.9 \times 10^{12} M_\odot$ and

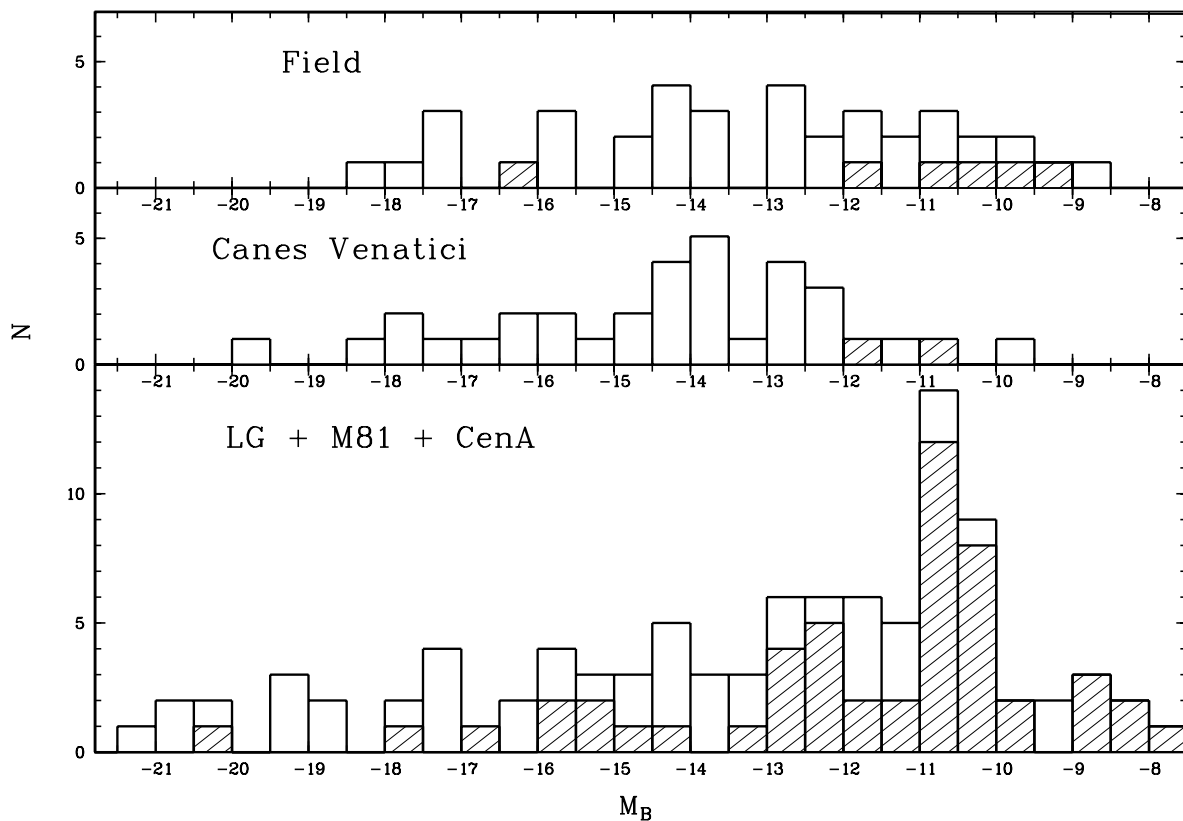


Fig. 5. The luminosity function of 34 CVnI cloud galaxies (middle histogram), 38 nearby field galaxies (upper histogram) and 96 galaxies situated in the LG, the M81 group, and the CenA group. E and dSph galaxies are shaded.

Table 3. Distance moduli for 19 galaxies in Canes Venatici derived from their brightest stars (BS) and RGB stars.

Galaxy	$(m - M)_{BS}$	$(m - M)_{RGB}$	difference
UGC 6541	27.73	27.95	-0.22
NGC 3738	27.73	28.45	-0.72
NGC 3741	27.70	27.41	0.29
UGC 6817	27.97	27.11	0.86
NGC 4214	28.06	27.34	0.72
UGC 7298	29.67	28.12	(1.55)
NGC 4244	28.28	28.26	0.02
NGC 4395	28.13	28.32	-0.20
UGC 7559	27.97	28.44	-0.47
UGC 7559	28.53	28.44	0.09
UGC 7577	28.42	27.02	(1.40)
NGC 4449	27.33	28.12	-0.79
UGC 7605	28.24	28.23	0.01
UGCA 290	27.20	29.13	(-1.93)
IC 3687	27.37	28.30	-0.93
UGC 8308	27.85	28.11	-0.26
UGC 8320	28.01	28.18	-0.17
NGC 5204	28.46	28.34	0.12
UGC 8651	27.66	27.39	0.27
UGC 8833	27.53	27.52	0.01

$M_{orb}/L_B = 88 M_{\odot}/L_{\odot}$. Both estimates are in satisfactory agreement with the mass-to-luminosity ratio, $M_{vir}/L_B = 93 M_{\odot}/L_{\odot}$ obtained by Tully (1987) for 22 members of the CVnI cloud.

Based on the present (incomplete) data on galaxy distances, we may establish that the CVnI cloud extends in depth some 2.5–3.5 Mpc, namely, from $D_{min} = 2.5$ Mpc to $D_{max} = 5$ Mpc (via the TRGB method) or even to 6 Mpc via the less reliable distance estimates from the brightest stars. In the projection onto the sky the most distant CVnI members are situated at $R_p \sim 1.4$ Mpc from the center. Hence, the CVnI cloud is a system slightly elongated in space along the line of sight.

It should be emphasized that such an extended complex of galaxies with a low velocity dispersion (only 50 km s^{-1}) has not yet reached the virialized state. The “crossing time” of the CVnI cloud defined as $T_{cross} = \langle R_p \rangle / \sigma_v$ is 15 Gyr, comparable to the cosmic expansion time. Consequently, the derived estimates of the virial/orbital mass should be used with great caution.

What is the dynamical state of the CVnI cloud? Is it a semi-virialized system or a structure taking part in the free Hubble flow? Figure 6 presents the distribution of galaxies in the CVnI region according to their distances and radial velocities. Here the galaxies with accurate distance estimates are shown by filled circles, and the galaxies with distances known only via the brightest stars are indicated by crosses. Four luminous galaxies with $M_B < -18$ mag are shown by filled squares. The straight line that passes the foreground objects KK 230, DDO 187, and UGC 8508, and the background galaxies UGCA 290, NGC 4258, and NGC 5194/95, fits a Hubble constant $H = 71 \text{ km s}^{-1} \text{ Mpc}^{-1}$. The CVnI centroid position is indicated by an open box whose sides correspond to

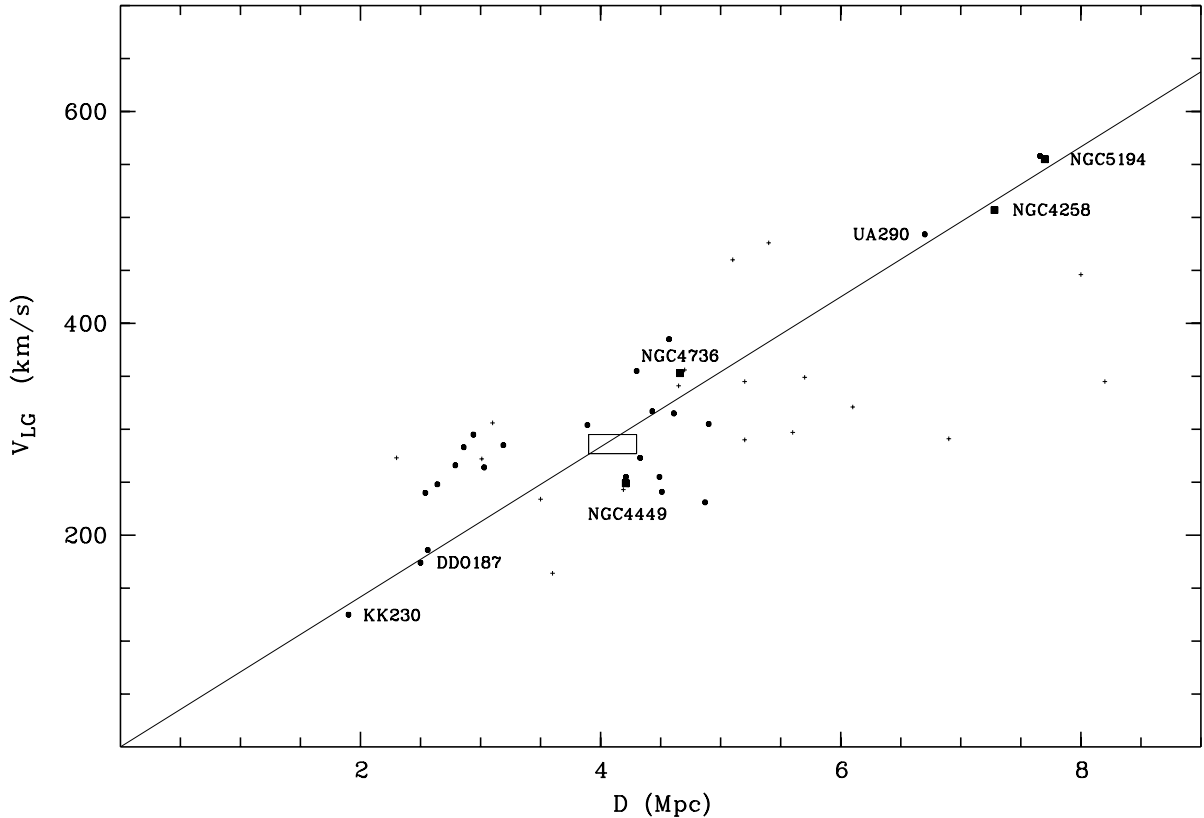


Fig. 6. Velocity-distance relation for galaxies in the CVn I region. The galaxies with accurate distance estimates are indicated by filled circles. The most luminous of them are shown as filled squares. The galaxies with distances estimated via the brightest stars are marked by crosses. The straight line corresponds to the Hubble constant $H_0 = 71 \text{ km s}^{-1} \text{ Mpc}^{-1}$. Position of the CVn I centroid is shown as an open box with sides equal to $1\text{-}\sigma$ errors of the mean distance and velocity.

the $1\text{-}\sigma$ errors of the mean distance and velocity. From the data we conclude that the peculiar velocity of the centroid of the CVn I cloud does not exceed the error of its determination, $\sim 20 \text{ km s}^{-1}$. This result seems to be not trivial, because of the existence of the Virgo-centric flow (Kraan-Korteweg 1986) can generate significant deviations from the pure Hubble flow on a scale of $\sim 5 \text{ Mpc}$.

The behavior of the members of the CVn I cloud in Fig. 6 reveals an interesting feature: all the galaxies at the front of the cloud are situated above the Hubble regression line. That may be caused by the differential motion of the peripheral galaxies towards the cloud center at a velocity of $\sim 65 \text{ km s}^{-1}$. In the case of spherical symmetry, a similar motion of more distant cloud members towards its center (i.e., towards us) is expected (Tonry et al. 2000). Unfortunately, the distances to galaxies at the back of the cloud are known so far only with large errors, and the suspected “back-flow” effect turns out to be very noisy. But we believe that more accurate distance measurements for a dozen galaxies on the back of the cloud can easily clarify whether the backflow effect exists or not.

Thus, returning to the question about the dynamical state of the CVn I cloud, we suggest that the complex of predominantly irregular galaxies shows some signs of deviation from the free Hubble expansion. But it seems to be very far from the virialized state. Presumably evolving systems like the CVn I cloud,

UMa cloud, and the Cancer cluster are a common feature of the large scale structure of the universe.

It should also be noted that in the CVn I region there are some galaxies (UGC 7131, NGC 4150, KK 127, and UGC 7949) with radial velocities of $100\text{--}350 \text{ km s}^{-1}$, but with distance estimates in the range of $(10\text{--}20) \text{ Mpc}$. These objects tend to be concentrated on the southern side of the cloud, closer to the Virgo cluster outskirts, and their low radial velocities may be caused by large peculiar motions with respect to the Virgo core.

6. Concluding remarks

As was noted above, the CVn I cloud is a scattered system elongated towards the Local Group. Together with the LG and the loose group in Sculptor, aligned along the line of sight, the CVn I cloud consists of an amorphous filament of $\sim 10 \text{ Mpc}$ in length. We estimated the excess of the number of galaxies in the CVn I cloud to be $(N - \langle N \rangle) / \langle N \rangle \sim 7$. Because the complex is populated predominantly by dwarf galaxies, the overdensity of the CVn I in its luminosity turns out to be lower, $(\rho_{\text{lum}} - \langle \rho_{\text{lum}} \rangle) / \langle \rho_{\text{lum}} \rangle \sim 4$. Here we adopted that the space volume of the CVn I is 21 Mpc^3 , and the mean luminosity of 1 Mpc^3 is $2 \times 10^8 L_\odot$ (Bahcall et al. 1995).

Remarkably, the mass estimates for the cloud, derived via orbital and virial motions and being distributed over the 21 Mpc^3 volume, yield an average density of dark matter $0.62\rho_c$ and $1.17\rho_c$, respectively, where $\rho_c = 1.0 \times 10^{-29} \text{ g/cm}^3$ is the critical density with $H_0 = 70 \text{ km s}^{-1} \text{ Mpc}^{-1}$.

The large crossing time for the CVn I cloud (15 Gyr), the low content of dSphs, the almost primordial shape of the LF indicate that the CVn I complex is in a transient state not so far from the pure Hubble flow. We hope that future accurate distance measurements of about 20–30 members of the cloud in a fast snapshot survey with the Advanced Camera will give a complete and reliable basis of studying the dynamical evolution of the Canes Venatici complex.

Acknowledgements. Support for this work was provided by NASA through grant GO-08601.01-A from the Space Telescope Science Institute, which is operated by the Association of Universities for Research in Astronomy, Inc., under NASA contract NAS5-26555. This work was partially supported by RFBR grant 01-02-16001 and DFG-RFBR grant 02-02-04012. D.G. gratefully acknowledges support from the Chile *Centro de Astrofísica* FONDAP No. 15010003. D.G. kindly acknowledges support from ESO as a Visiting Astronomer which allowed him to work on this paper.

The Digitized Sky Surveys were produced at the Space Telescope Science Institute under U.S. Government grant NAG W-2166. The images of these surveys are based on photographic data obtained using the Oschin Schmidt Telescope on the Palomar Mountain and the UK Schmidt Telescope. The plates were processed into the present compressed digital form with permission of these institutions.

This project made use of the NASA/IPAC Extragalactic Database (NED), which is operated by the Jet Propulsion Laboratory, Caltech, under contract with the National Aeronautics and Space Administration.

References

- Aparicio, A., Tikhonov, N., & Karachentsev, I. 2000, *AJ*, 119, 177
 Arp, H. 1966, *Atlas of Peculiar Galaxies*, *ApJS*, 14, 1
 Bahcall, N. A., Lubin, L. M., & Dorman, V. 1995, *ApJ*, 447, L81
 Bellazzini, M., Ferraro, F. R., & Pancino, E. 2001, *ApJ*, 556, 635
 Bicay, M. D., & Giovanelli, R. 1987, *AJ*, 93, 1326
 Bresolin, F., Capaccioli, M., & Pionto, G. 1993, *AJ*, 105, 1779
 Bureau, M., Freeman, K. C., Pfitzner, D. W., & Meuer, G. R. 1999, *AJ*, 118, 2158
 Carignan, C., & Beaulieu, S. 1989, *ApJ*, 347, 760
 Crone, M. M., Schulte-Ladbeck, R. E., Greggio, L., & Hopp, U. 2002, *ApJ*, 567, 258
 Da Costa, G. S., & Armandroff, T. E. 1990, *AJ*, 100, 162
 Dolphin, A. E. 2000a, *PASP*, 112, 1383
 Dolphin, A. E. 2000b, *PASP*, 112, 1397
 de Vaucouleurs, G. 1975, in *Galaxies and the Universe*, ed. A. Sandage, M. Sandage, & J. Kristian (Chicago, Univ. of Chicago Press), p. 557
 Ferrarese, L., Mould, J. R., Kennicutt, R. C., Jr., et al. 2000, *ApJ*, 529, 745
 Georgiev, Ts. B., Karachentsev, I. D., & Tikhonov, N. A. 1997, *Lett. Astron. Zh.*, 23, 586
 Grebel, E. K., et al. 2000, in *Stars, Gas, and Dust in Galaxies: Exploring the Links*, ed. D. Alloin, K. Olsen, & G. Galaz (Provo: ASP), ASP Conf. Ser., 221, 147
 Hopp, U., & Schulte-Ladbeck, R. E. 1995, *A&AS*, 111, 527
 Haynes, M., & Giovanelli, R. 1991, *ApJS*, 77, 331
 Huchtmeier, W. K., & Karachentsev, I. D. 2002, *A&A*, submitted
 Huchtmeier, W. K., Karachentsev, I. D., Karachentseva, V. E., & Ehle, M. 2000, *A&AS*, 141, 469
 Karachentsev, I. D., Karachentseva, V. E., Dolphin, A. E., et al. 2000, *A&A*, 363, 117
 Karachentsev, I. D., Sharina, M. E., Dolphin, A. E., et al. 2001, *A&A*, 375, 359
 Karachentsev, I. D., Sharina, M. E., Dolphin, A. E., et al. 2002a, *A&A*, 385, 21
 Karachentsev, I. D., Dolphin, A. E., Geisler, D., et al. 2002b, *A&A*, 383, 125
 Karachentsev, I. D., Sharina, M. E., Makarov, D. I., et al. 2002c, *A&A*, 389, 812
 Karachentseva, V. E., & Karachentsev, I. D. 1998, *A&AS*, 127, 409
 Karachentsev, I. D., & Drozdovsky, O. I. 1998, *A&AS*, 131, 1
 Karachentsev, I. D., & Tikhonov, N. A. 1994, *A&A*, 286, 718
 Karachentsev, I. D., Kopylov, A. I., & Kopylova, F. G. 1994, *Bull. Spec. Astrophys. Obs.*, 38, 15
 Karachentsev, I. D. 1966, *Astrofizika*, 2, 81
 Kraan-Korteweg, R. C. 1986, *A&AS*, 66, 255
 Lee, M. G., Freedman, W. L., & Madore, B. F. 1993, *ApJ*, 417, 553
 Limber, D. N., & Mathews, W. G. 1960, *ApJ*, 132, 286
 Maiz-Apellaniz, Cieza L., & MacKenty, J. W. 2002, *AJ*, 123, 1307
 Makarova, L. 1999, *A&AS*, 139, 491
 Makarova, L., Karachentsev, I., Takalo, L. O., Heinamaki, P., & Valtonen, M. 1998, *A&AS*, 128, 459
 Makarova, L. N., Karachentsev, I. D., & Georgiev, Ts. B. 1997, *Lett. Astron. Zh.*, 23, 435
 Paturel, G., Bottinelli, L., Di Nella, H., et al. 1996, *Catalogue of Principal Galaxies, (PGC-ROM)*, Saint-Genis Laval, Observatoire de Lyon
 Prugniel, P., & Heraudeau, P. 1998, *A&AS*, 128, 299
 Rozanski, R., & Rowan-Robinson, M. 1994, *MNRAS*, 271, 530
 Sakai, S., Madore, B. F., & Freedman, W. L. 1996, *ApJ*, 461, 713
 Salaris, M., & Cassisi, S. 1997, *MNRAS*, 289, 406
 Sandage, A., & Tammann, G. A. 1982, *ApJ*, 256, 339
 Schlegel, D. J., Finkbeiner, D. P., & Davis, M. 1998, *ApJ*, 500, 525
 Seitzer, P., Grebel, E. K., Dolphin, A. E., et al. 1999, *AAS*, 195, 0801
 Sharina, M. E., Karachentsev, I. D., & Tikhonov, N. A. 1999, *Lett. Astron. Zh.*, 25, 380
 Tikhonov, N. A., & Karachentsev, I. D. 1998, *A&AS*, 128, 325
 Tonry, J. L., Dressler, A., Blakeslee, J. P., et al. 2001, *ApJ*, 546, 681
 Tonry, J. L., Blakeslee, J. P., Ajhar, E. A., & Dressler, A. 2000, *ApJ*, 530, 625
 Tully, R. B., Somerville, R. S., Trentham, N., & Verheijen, M. A. 2002, *ApJ*, 569, 573
 Tully, R. B., Verheijen, M. A., Pierce, M. J., et al. 1996, *AJ*, 112, 2471
 Tully, R. B. 1988, *Nearby Galaxy Catalog* (Cambridge Univ. Press)
 Tully, R. B. 1987, *ApJ*, 321, 280
 Udalski, A., Wyrzykowski, L., Pietrzynski, G., et al. 2001, *Acta Astron.*, 51, 221
 Vennik, J. 1984, *Tartu Astron. Obs. Publ.*, 73, 1